

## Time evolution effect on the scour characteristics downstream of the sluice gate with the submerged hydraulic jump in a laboratory model

Ali Mahdian Khalili <sup>1</sup>  
Mehdi Hamidi <sup>2</sup>

### Abstract

Sluice gates are utilized in dams and irrigation channels as regulating structures in the channel have the role of regulating the water level for proper water intake of upstream intakes. As high velocity and energy of the flow issuing from these hydraulic structures scour occurred in erodible downstream beds. Occurrence of the hydraulic jump is very possible, and when it forms, therefore the necessity of investigating the flow condition increases. The scouring phenomenon is a time evolution and a long-time procedure. This research focused on time effects on experimental data received by a sediment bed profiler at different times from the experimental setup conducted in a laboratory. The maximum scour depth ( $d_{se}$ ), the maximum dune height ( $h_d$ ), the horizontal distance of the maximum scour depth from the beginning of the sedimentary bed ( $x_{se}$ ), and the horizontal distance of the maximum dune height from the beginning of the sedimentary bed ( $x_d$ ) were investigated. Laboratory observations show that the extension of the location of the maximum scour depth and the maximum height of the dune formed with time is evident. The laboratory data for the dimensionless conditions of 4 scour profiles characteristics including  $d_{se}/b_0$ ,  $h_d/b_0$ ,  $x_{se}/b_0$ , and  $x_d/b_0$  were analyzed by the nonlinear regression method, and separate equations were proposed for each characteristic.  $RMSE=0.045$ ,  $0.0677$ ,  $0.358$ , and  $2.146$  respectively, and the  $R^2=0.996$ ,  $0.975$ ,  $0.974$ , and  $0.977$  respectively.

**Keywords:** Scour equilibrium time, Scour profile, Submerged jump, Gate opening, Experimental model.

Received: 16 April 2023; Accepted: 25 July 2023

<sup>1</sup> Faculty of Civil Engineering, Babol Noshirvani University of Technology, Babol, Mazandaran, Iran.

<sup>2</sup> Faculty of Civil Engineering, Babol Noshirvani University of Technology, Babol, Mazandaran, Iran.  
Email: hamidi@nit.ac.ir , Tel.: 0098 011 35501520 (Corresponding author)



## 1. Introduction

The interaction between water flow and bed materials and the river walls or erodible irrigation channels leads to the phenomenon of scouring. This process begins when the fluid shear stress becomes more than the critical shear stress of the granular bed materials. The variations in the bed form around hydraulic structures when scour occurs may influence the performance of hydraulic structures including bridge piers, coastal piers, culverts, pipelines, stilling basins in dams, flow control structures such as weirs and gates in dams, and irrigation channel systems. In particular, in the investigation of the flow passing through the flow regulating gates, according to the high velocity and energy issuing from the jet flow, the occurrence of a hydraulic jump is probable. The simultaneous occurrence of hydraulic jump and sediment transport phenomena adds to the complexity of the hydraulic behavior of the flow. Considering the importance of the primary and secondary effects of erosion on the hydraulic behavior of the passing flow and also its effects on the performance of the gate structure, the investigation of scour caused by the jets issuing through the gates has attracted the opinion of researchers and designers of hydraulic structures. These studies include laboratory research to comprehend the hydraulic characteristics of the scour and the development of erosion prediction models for optimal design. In the following, the evolution of researchers' studies on the erosion of sedimentary beds downstream of sluice gates is reviewed.

Scour downstream of sluice gates is an evolutionary and time-dependent process, and time is an effective factor in the characteristics of the scour profiles. Balachandar et al. [1] conducted a laboratory study of a 2D local scour hole that forms downstream of the submerged sluice gate for different tailwater depths by using a video imaging method and a laser-Doppler anemometer. Their observations indicated that the flow field is dynamic and varied with time.

The tailwater depth and the Froude number are the hydraulic parameters that affect the characteristics of downstream scour jet issuing through the sluice gates, which have been investigated in various studies in the laboratory. Without a protective apron, when the tailwater is deep or shallow, the characteristics of the equilibrium condition of the scour profile are dependent on the densimetric Froude number [2]. Farhodi and Khalili Shayan [3] studied the local scour after the reverse stilling basin caused by a submerged wall jet issuing the sluice gate. They found that the scour profiles in each slope of the bed followed the similarity of the shape and the evolution of the longitudinal scour profiles and the scour volume in the granular bed was increasing in proportion to the slope of the basin.

The physical properties of the sedimentary bed are effective parameters in the scour process, which are generally investigated in the form of sediment grain size and characteristics of the granular curve. Kells et al. [4] conducted a laboratory investigation to evaluate the influence of sediment particle size on the dynamics of the scour process after a submerged sluice gate. They used 36 laboratory experiments on 4 gradations of non-cohesive bed materials under flow conditions with different flow velocities and depths to study the scouring process. Dey and Sarkar [5,6] studied the scour of non-cohesive uniform and non-uniform sedimentary beds downstream of the apron with a submerged horizontal jet issuing through the sluice gate opening. In the scouring process and the profiles (including the dune downstream of the scour hole) at various times, they followed a specific geometrical similarity and proposed it by combining two multinomials. They used different tailwater depths and measured scour depth at various times. The time variation of the scour depth was provided by an exponential law that the time scale increased linearly with the densimetric Froude number.

One of the countermeasures against erosion caused by the flow of high-velocity jets issuing from hydraulic structures such as sluice gates is the use of a rigid apron after the jet and before

the sedimentary bed. With the installation of the apron, due to the high energy and insufficient consumption of energy, local scour occurs downstream of the apron and in the erodible bed. Nik Hassan and Narayanan [7] conducted a laboratory study to measure the scour profile downstream of the jet issuing from the gate opening on the rigid apron. By drawing the average velocity distribution curves in rigid aprons that modeled the shape of the scour hole, they found that the curves are similar. Rajaratnam and Aderbigbe [8] presented a laboratory method to reduce scour downstream of vertical gates. They placed a reticulated plate on the beginning of the sedimentary bed downstream of the gate and conducted experiments using three sizes of sand grains and three reticulated plates with different designs. They found that apparently, the installation of the reticulated plates diverts the high velocity from the erodible bed and reduces scour depth significantly. He has measured the longitudinal distribution of velocity with an erodible bed in one of the experiments in an approximate condition, to obtain a better understanding of the erosion decrease process. Hamidifar et al. [9] determined the factors affecting the scour profiles downstream of the apron in an experimental study and formed effective dimensionless parameters with dimensional analysis. They are the dimensionless curves of scour profile parameters such as the maximum scour depth ( $d_{se}$ ) and its location ( $x_{se}$ ), the value of bed scour in the vicinity of the apron, the maximum expansion of the hole, the horizontal distance from the end of the apron to the crest of the dune ( $x_d$ ) and its height ( $h_d$ ) and compared the results with previous studies. Hamidifar et al. [10,11] studied the effects of using a bed sill downstream of the apron in reducing scour and evaluating its effect at different locations in the sedimentary bed. By examining the changes in the profile of the scour hole, they observed that  $d_{se}$  can be reduced by 95%. They also investigated the effects of the combination of bed sill and riprap, to reduce  $d_{se}$  in the vicinity of the horizontal rigid apron in laboratory conditions. Chaudhary et al. [12] used a corrugated rigid apron upstream of the sedimentary bed, which decreases  $d_{se}$  by about 80%. Ghassemi et al. [13,14] applied geonets and synthetic fibers as a new approach to decrease local scour downstream of a sluice gate with a rigid apron.

Predicting the scour hole characteristics downstream of the jets with acceptable accuracy is required [15]. Chang et al. [16] investigated the mechanism for the occurrence of equilibrium and non-equilibrium scour holes and resulted that at equilibrium condition, the location of the re-attachment point is significantly affected by the flow discharge. Mostaani and Azimi [17] used the bed shear stress and scour profile curvature (SSC model) to estimate the scour profile in temporal and equilibrium phases.

It could be understood from reviewing previous studies that the focus of laboratory models is on determining  $d_{se}$  and implementing countermeasures to reduce it. Maximum scour depth ( $d_s$ ) was investigated during the equilibrium scour condition and it was only allocated to the equilibrium scour curves. Therefore, in this research, while examining the  $d_s$  during the equilibrium time and its evolution, other characteristics of the scour profile, such as the dune height ( $h_d$ ) and its horizontal location ( $x_d$ ), and its horizontal location of  $d_{se}$  ( $x_{se}$ ), are investigated. Also, with nonlinear regression analysis, some equations and graphs are presented to predict the varied behavior of scour profile characteristics with time.

## 2. materials and methods

### 2.1. Laboratory model setup

The tests of this research were carried out in the hydraulic laboratory flume of BNTU with a rectangular cross-section. Flume is 10 meters long, 0.3 meters wide, and 0.38 meters high, which can adjust the bed slope from 0 to 0.04. This flume has glass walls and a PVC floor (figure 1). When the pump turns on and the discharge valve is opened, the water comes from the upstream tank to the channel and then stores in the downstream tank and transports to the upstream tank through the connecting valve and transmission pipe, and this cyclic process will continue as long as the pump is on. In irrigation channels, the slope of the channel bed varies between 0.0005 and 0.006 [18]. The slope of the channel bed is considered constant and equal to 0.005 in the tests. A 0.008-meter-thick metal gate is used, which is screwed on the channel rail by holding clamps and a vertical plate that can adjust the vertical gate opening. A rigid apron is used with a height equal to the depth of the sedimentary bed and a length of 2 meters, which continues for 1.5 meters after the gate opening to protect the sedimentary bed from erosion. The floor structure is made of PVC based on the mentioned dimensions. After the apron, the 3-meter-long recess is filled with sediment to a depth of 0.2 meters, and at the end of the bed, a sediment trap with the sedimentary bed thickness is placed to store and trap the sediments. The flume has a tailgate at its end that can be used to adjust the tailwater depth and also trap sediments. Figure 2 shows the laboratory model and the structures installed on the flume, which include a sluice gate, a rigid apron, a sediment bed, and a sediment trap.



Figure 1. Laboratory flume



Figure 2. Experimental model and installed structures

Breusers and Raudkivi [19] defined a threshold value of  $\sigma_g=1.35$  for non-uniform granulation. For the present study, sand with sedimentary characteristics according to Table 1 was selected and graded for the sedimentary bed.  $d_i$  is the grain size that  $i$  percentage of sedimentary materials are smaller than, and  $\sigma_g$  is the geometric standard deviation of sediment particles. Figure 3 shows the granulation curve of the selected materials.

Table 1. Sedimentary parameters of the sand bed

| $d_{10}$ (mm) | $d_{16}$ (mm) | $d_{50}$ (mm) | $d_{60}$ (mm) | $d_{84}$ (mm) | $\sigma_g$ |
|---------------|---------------|---------------|---------------|---------------|------------|
| 1.15          | 1.24          | 1.6           | 1.72          | 2.27          | 1.35       |

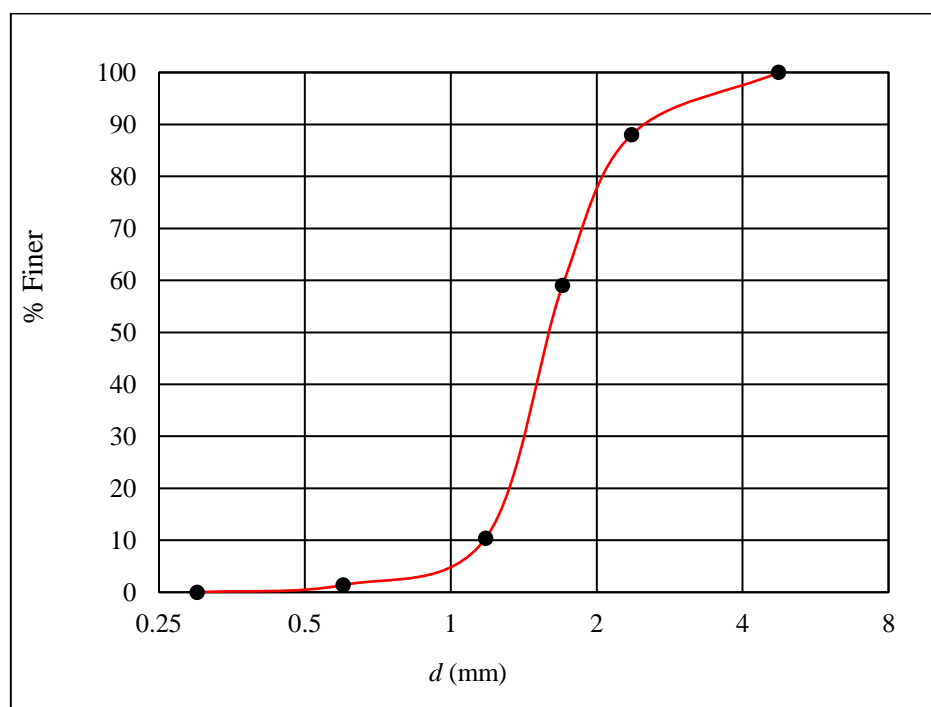


Figure 3. Granulation curve of bed materials

Two different hydraulic conditions have been implemented according to Table 2 to evaluate the efficiency of time evolution on the scour profiles downstream of the sluice gate. In this table,  $b_0$  is the opening of the valve in meters,  $h_t$  is the tailwater in meters,  $U$  is the jet velocity issuing from the gate opening in meters per second, and  $Fr$  is the Froude number of a jet issuing through the sluice gate and  $F_d$  is densimetric Froude number.

Table 2. Hydraulic condition setup of experimental model

| Case | $b_0$ (m) | $h_t$ (m) | $U$ (m/s) | $Fr$ | $F_d$ |
|------|-----------|-----------|-----------|------|-------|
| A    | 0.015     | 0.095     | 0.8       | 1.47 | 4.97  |
| B    | 0.020     | 0.095     | 1.9       | 3.5  | 11.81 |

## 2.2. Equilibrium time scour

When the flow issuing through the sluice gate collides with the sediment particles, a large number of sediment particles are rises and moved downstream, and the scour process begins. During this procedure, a scour hole and a dune are generated. According to the observations of previous researchers, this process includes three phases initial, development, and equilibrium [20-22]. In the initial phase, the scour speed is too fast, but in the development phase, the rate of scour is relatively slower. Finally, after a long time, upon reaching the equilibrium scour hole, the velocity decreases and finally approaches zero [20]. In the initial phase, the scour depth reaches approximately 70% of the ultimate scour depth, while the time of this stage is less than 10% of the equilibrium time. In the second phase, the scour hole is developed and the scour depth reaches approximately 90% of the final scour depth. During this stage, the scour procedure developed gently and for a period of approximately 40% of the final equilibrium time. In the

equilibrium phase, the scour hole evolves only 10%, and its time is approximately 50% of the total time of the three phases of the scour process [22]. Reaching the approximate conditions of equilibrium scour is one of the important things in laboratory implementations, so the time variation graph of the scour hole should be considered. The bed profiler of the flume is used, to measure the scour depth of the hole at a desired time, which has the accuracy of measuring the depth up to 1 mm. By drawing the profiles of the time evolution of bed scour, when the profiles coincide and its changes approach zero, it can be considered as the equilibrium scour time and the experiment finished.

### 2.3. Extracted parameters of scour profile

In this study, the length of the sedimentary bed is considered to be 3 meters so that it is possible to investigate the scour profiles of the hole and dune simultaneously. The studied sedimentary characteristics include the maximum depth ( $d_{se}$ ) and its longitudinal distance from the end of the apron ( $x_{se}$ ), the maximum height of the dune ( $h_d$ ), and the horizontal distance from the end of the apron to its location ( $x_d$ ) that is presented in figure 4. These values are taken with the bed profiler of the flume during the experiment and the required times.

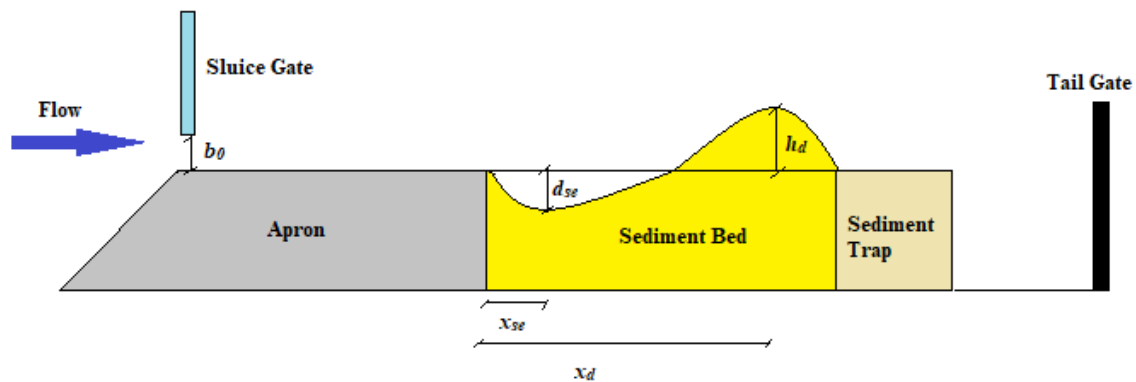


Figure 4. Extracted sedimentary parameters of scour profile

### 3. Results and discussion

Table 3 shows the results of scour profile characteristics extracted at different times from 5 to 1440 minutes under different conditions of densimetric Froude numbers 4.97, and 11.81. In this section, the values of the effects of time on the different characteristics of the erosion profile are interpreted. In the end, based on the laboratory data, 4 separate relationships are proposed for the mentioned characteristics, and their scope of application is presented.



**Table 3. Time evolution parameters of scour profiles**

| <b>Test number</b> | <b><math>F_{d50}</math></b> | <b><math>t</math> (min)</b> | <b><math>d_{se}</math> (mm)</b> | <b><math>h_d</math> (mm)</b> | <b><math>x_{se}</math> (mm)</b> | <b><math>x_d</math> (mm)</b> |
|--------------------|-----------------------------|-----------------------------|---------------------------------|------------------------------|---------------------------------|------------------------------|
| A1                 | 4.97                        | 5                           | 26                              | 13                           | 10                              | 320                          |
| A2                 | 4.97                        | 30                          | 32                              | 15                           | 10                              | 370                          |
| A3                 | 4.97                        | 60                          | 33                              | 16                           | 10                              | 420                          |
| A4                 | 4.97                        | 120                         | 34                              | 16                           | 10                              | 480                          |
| A5                 | 4.97                        | 180                         | 35                              | 17                           | 20                              | 500                          |
| A6                 | 4.97                        | 240                         | 36                              | 17                           | 20                              | 550                          |
| A7                 | 4.97                        | 300                         | 37                              | 18                           | 20                              | 570                          |
| A8                 | 4.97                        | 360                         | 38                              | 19                           | 20                              | 580                          |
| A9                 | 4.97                        | 420                         | 39                              | 19                           | 30                              | 620                          |
| A10                | 4.97                        | 480                         | 39                              | 20                           | 30                              | 650                          |
| A11                | 4.97                        | 540                         | 40                              | 20                           | 30                              | 680                          |
| A12                | 4.97                        | 600                         | 40                              | 21                           | 40                              | 700                          |
| A13                | 4.97                        | 660                         | 41                              | 22                           | 40                              | 720                          |
| A14                | 4.97                        | 720                         | 41                              | 22                           | 40                              | 750                          |
| A15                | 4.97                        | 780                         | 42                              | 23                           | 50                              | 760                          |
| A16                | 4.97                        | 840                         | 42                              | 23                           | 50                              | 770                          |
| A17                | 4.97                        | 900                         | 42                              | 24                           | 50                              | 780                          |
| A18                | 4.97                        | 960                         | 42                              | 24                           | 60                              | 790                          |
| A19                | 4.97                        | 1080                        | 43                              | 25                           | 60                              | 800                          |
| A20                | 4.97                        | 1200                        | 43                              | 25                           | 60                              | 810                          |
| A21                | 4.97                        | 1320                        | 43                              | 25                           | 60                              | 820                          |
| A22                | 4.97                        | 1440                        | 43                              | 25                           | 60                              | 820                          |
| B1                 | 11.81                       | 5                           | 48                              | 23                           | 20                              | 450                          |
| B2                 | 11.81                       | 30                          | 54                              | 28                           | 30                              | 520                          |
| B3                 | 11.81                       | 60                          | 57                              | 29                           | 30                              | 580                          |
| B4                 | 11.81                       | 120                         | 61                              | 30                           | 40                              | 680                          |
| B5                 | 11.81                       | 180                         | 64                              | 31                           | 40                              | 740                          |
| B6                 | 11.81                       | 240                         | 65                              | 32                           | 50                              | 780                          |
| B7                 | 11.81                       | 300                         | 66                              | 33                           | 50                              | 800                          |
| B8                 | 11.81                       | 360                         | 67                              | 34                           | 60                              | 830                          |
| B9                 | 11.81                       | 420                         | 67                              | 35                           | 60                              | 850                          |
| B10                | 11.81                       | 480                         | 68                              | 35                           | 70                              | 860                          |
| B11                | 11.81                       | 540                         | 68                              | 36                           | 70                              | 870                          |
| B12                | 11.81                       | 600                         | 69                              | 36                           | 80                              | 880                          |
| B13                | 11.81                       | 660                         | 69                              | 37                           | 90                              | 890                          |
| B14                | 11.81                       | 720                         | 70                              | 37                           | 100                             | 900                          |
| B15                | 11.81                       | 780                         | 70                              | 38                           | 110                             | 920                          |
| B16                | 11.81                       | 840                         | 71                              | 38                           | 110                             | 930                          |
| B17                | 11.81                       | 900                         | 71                              | 39                           | 120                             | 950                          |
| B18                | 11.81                       | 960                         | 71                              | 39                           | 120                             | 960                          |
| B19                | 11.81                       | 1080                        | 72                              | 40                           | 130                             | 980                          |
| B20                | 11.81                       | 1200                        | 72                              | 40                           | 130                             | 1030                         |
| B21                | 11.81                       | 1320                        | 72                              | 40                           | 130                             | 1030                         |
| B22                | 11.81                       | 1440                        | 72                              | 40                           | 130                             | 1030                         |

### 3.1. Effect of $t/t_e$ on $d_{se}$ and $h_d$

The time evolution and equilibrium scour conditions for each characteristic are presented in a separate graph. Figures 5 and 6 show the time evolution curves of  $d_{se}$  and  $h_d$ , respectively. The results show that at the beginning of the scouring time,  $d_{se}$  and  $h_d$  are high and include a significant part of the final value (more than 70%). Also, over time, the increasing rate of changes in  $d_{se}$  and  $h_d$  has reduced to the point where these changes approached zero and remain constant. This time will be the time of equilibrium. It can be observed that by comparing Figures 5 and 6, the sediment transport from the hole to the dune occurs, because, with the increase in  $d_{se}$ ,  $h_d$  also increases.

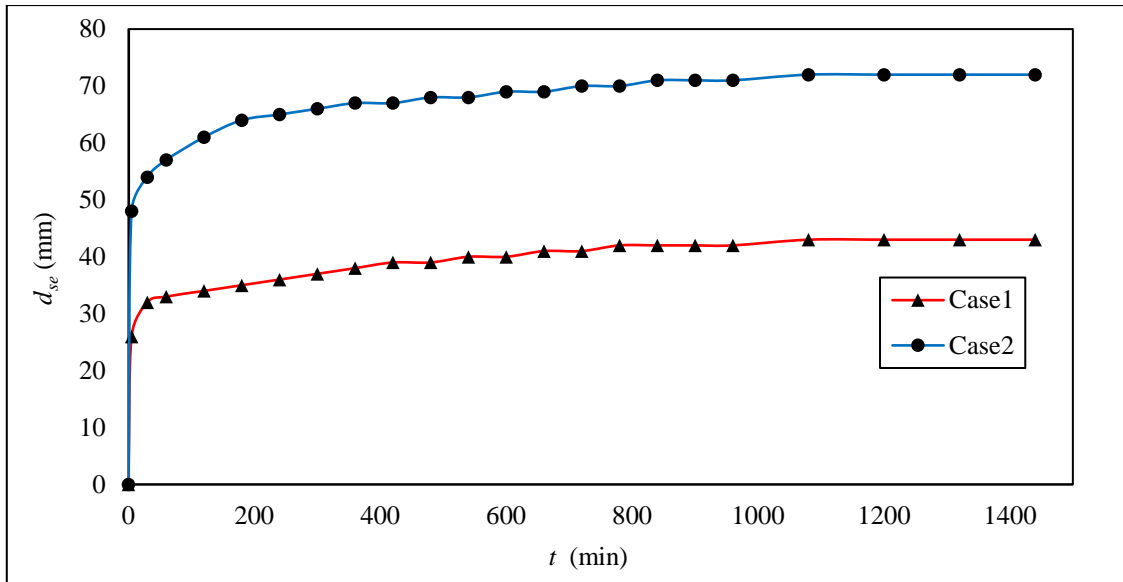


Figure 5. Time evolution of  $d_{se}$  of scour profile

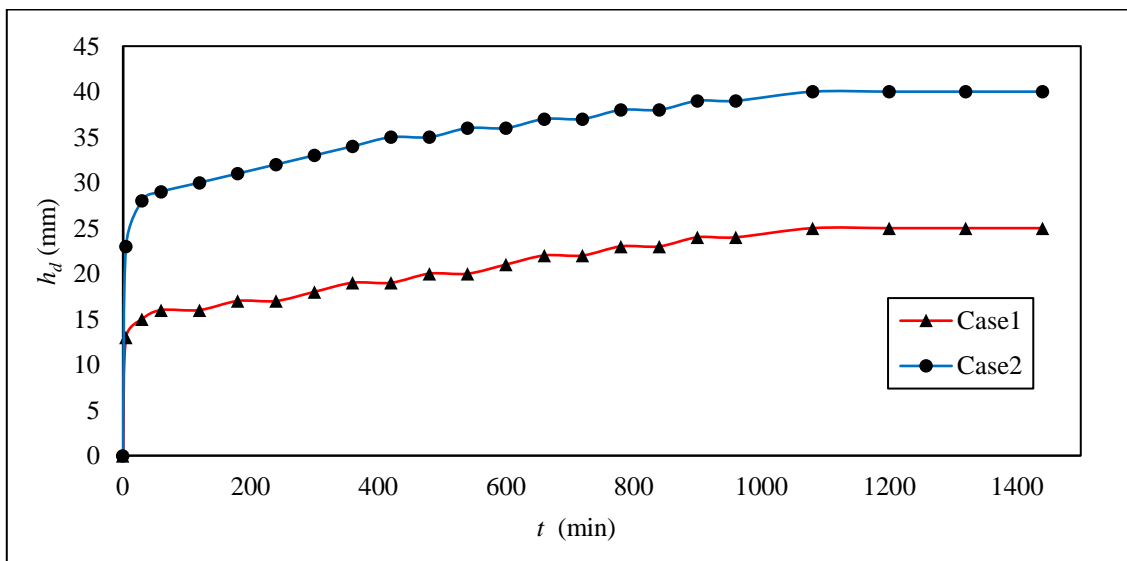


Figure 6. Time evolution of  $h_d$  of scour profile



Using the nonlinear regression method, an equation for predicting  $d_{se}$  with time evolution from the results obtained from the laboratory data is presented as Eq. 1.

$$\frac{d_{se}}{b_0} = 1.7948 \left(\frac{t}{t_e}\right)^{0.2923} (F_d)^{0.08} \quad (1)$$

Root mean square error ( $RMSE$ ) coefficient is used to determine the accuracy of the proposed equation, which is obtained from Eq. 2 [23].

$$RMSE = \sqrt{\frac{\sum_1^n (X_P - X_O)^2}{n}} \quad (2)$$

Where  $X_P$  is the predicted values,  $X_O$  is the observed values, and  $n$  is the number of data [24]. The prediction equation indicates that  $d_{se}/b_0$  has a direct relationship with  $F_d$  and  $t/t_e$ . By calculating the values of  $RMSE=0.045$  and  $R^2=0.996$ , a suitable match between the computational and laboratory data can be seen. Figure 7 indicates the range of changes of  $d_{se}/b_0$  observed compared to the predicted values from the proposed relationship.

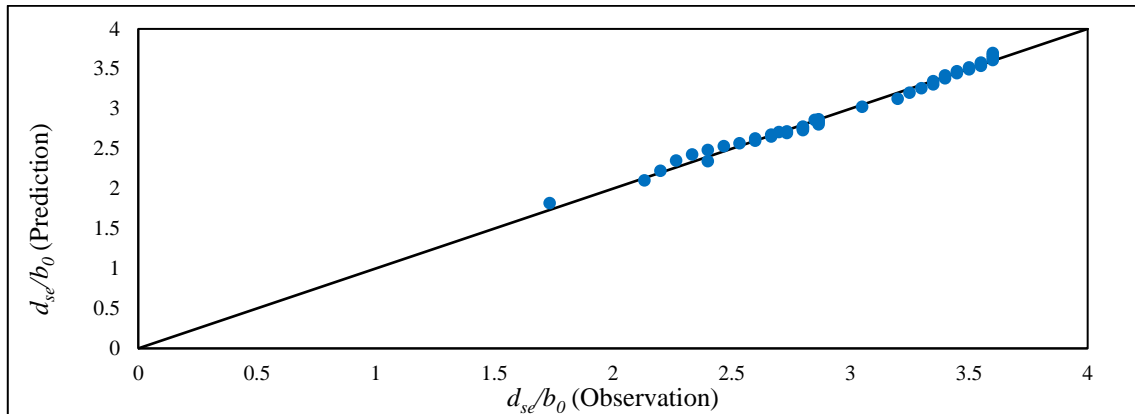


Figure 7. Changes of  $d_{se}/b_0$  (observed) to  $d_{se}/b_0$  (predicted)

An empirical equation for predicting the maximum dune height with time evolution from the results obtained from the laboratory data is presented as equation 3:

$$\frac{h_d}{b_0} = 1.0106 \left(\frac{t}{t_e}\right)^{0.2842} (F_d)^{0.1219} \quad (3)$$

It concluded that in equation 3,  $h_d/b_0$  has a direct proportion with the parameters  $F_d$  and  $t/t_e$ . The values of  $RMSE=0.0677$  and  $R^2=0.975$  show good compatibility between the computational and laboratory data. Figure 8 shows the range of  $h_d/b_0$  observed variation compared to the predicted values from the proposed relationship.

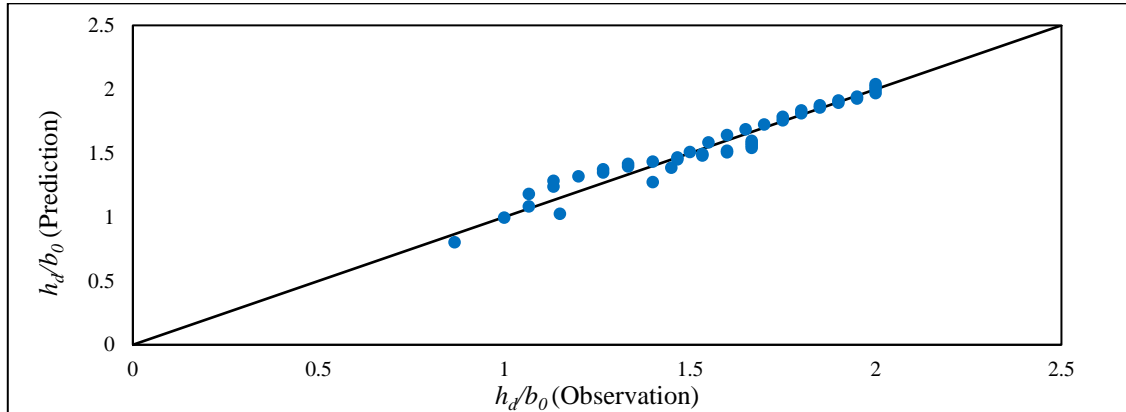
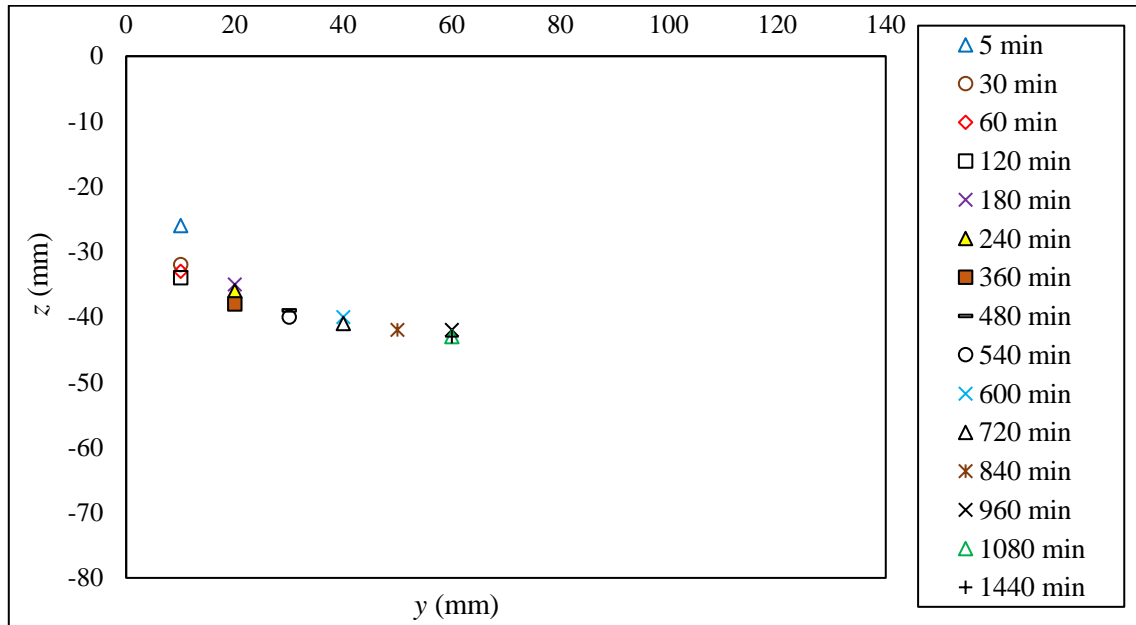


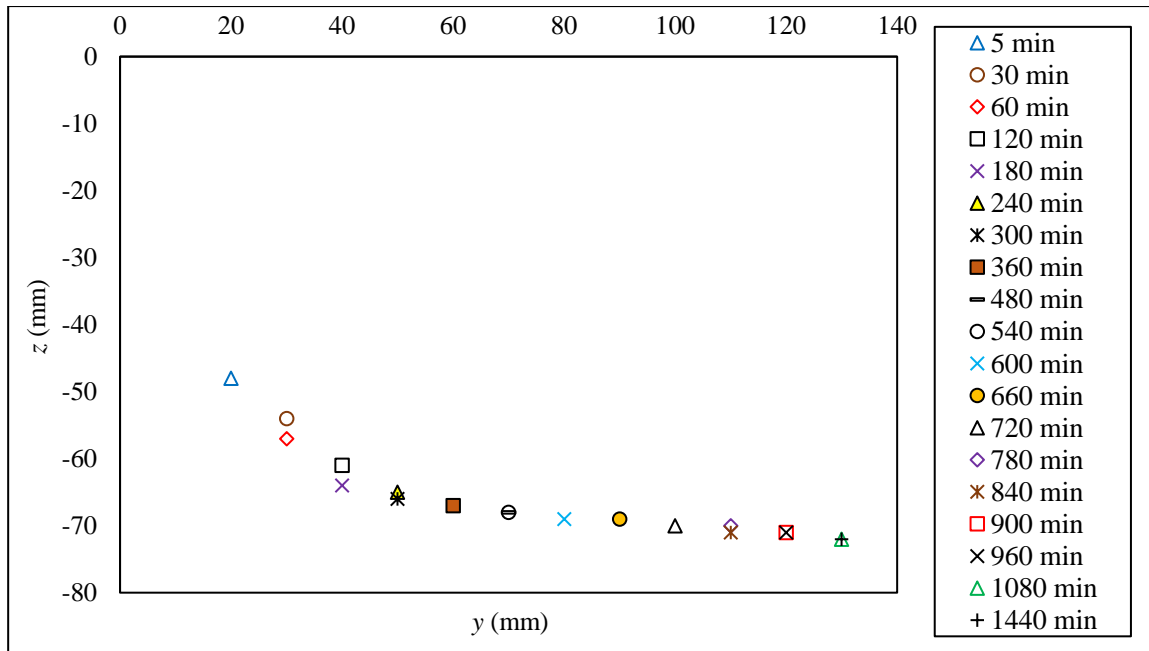
Figure 8. Changes of  $h_d/b_0$  (observed) to  $h_d/b_0$  (predicted)

### 3.2. Effect of $t/t_e$ on $x_{se}$ and $x_d$

Figures 9 (a) and (b) and figures 10 (a) and (b) show the time evolution curves of  $x_{se}$  and  $x_d$  for cases 1 and 2, respectively. It could be observed in Fig. 9 and Fig. 10, that with time, both the horizontal location of  $d_{se}$  and  $h_d$  move downstream, and the extension of the hole and the dune occurs. For case 1, where the velocity and Froude number of the jet are higher, the amount of this extension will be longer.

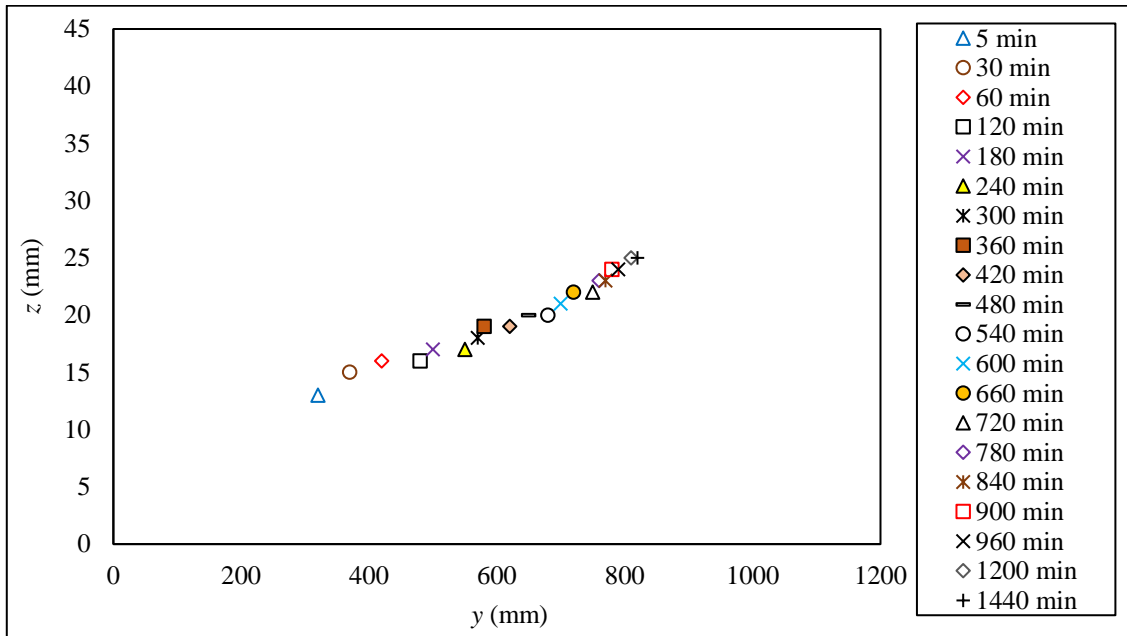


(a)

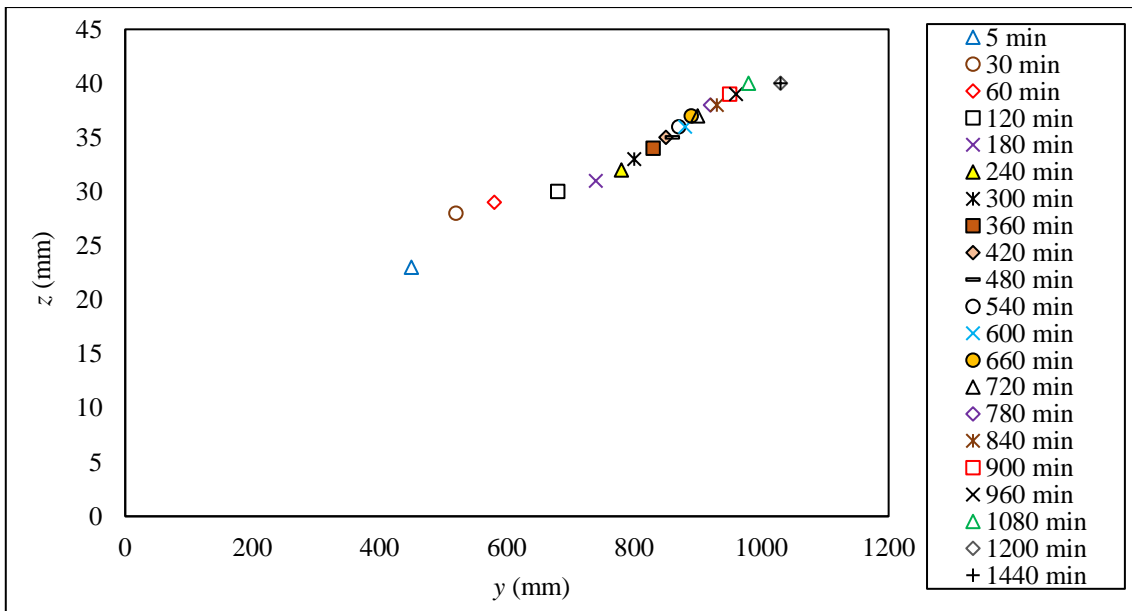


(b)

Figure 9. Time evolution of  $x_{se}$  (a)  $F_d=4.97$  (b)  $F_d=11.81$



(a)



(b)

**Figure 10. Time evolution of  $x_d$  (a)  $F_d=4.97$  (b)  $F_d=11.81$**

Equation 4 is proposed from the nonlinear regression analysis of the results obtained from the laboratory data, to estimate the longitudinal distance of the location of the maximum scour depth from the beginning of the bed with time evolution.

$$\frac{x_{se}}{b_0} = 1.7829 \left(\frac{t}{t_e}\right)^{0.5604} (F_d)^{0.5756} \tag{4}$$

It was figured out from equation 4, that  $x_{se}/b_0$  has a direct relationship with parameters  $F_d$  and  $t/t_e$ . The values of  $RMSE=0.358$  and  $R^2=0.974$  were calculated between the computational and laboratory data, which are good accuracy. Figure 11 presents the range of  $x_{se}/b_0$  observed variations compared to the predicted values from the provided equation.

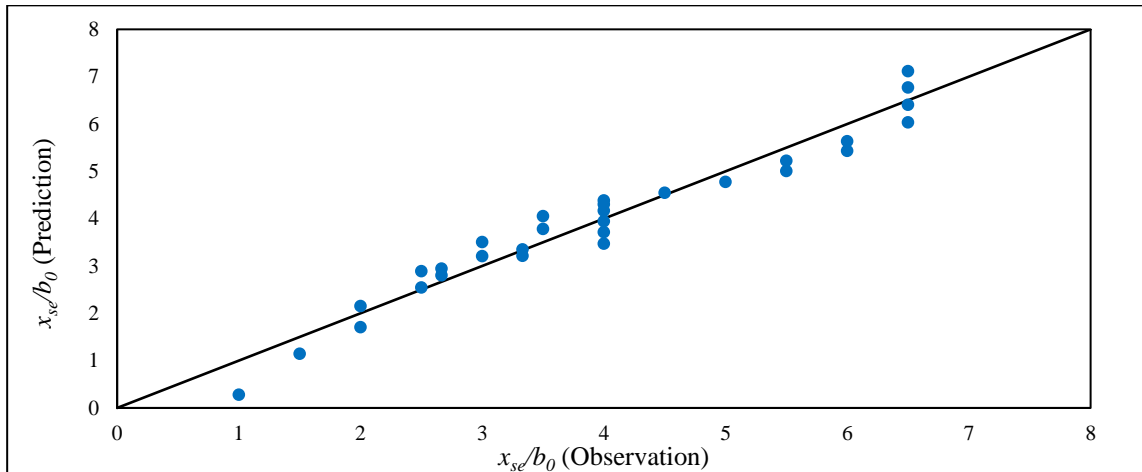


Figure 11. Changes of  $x_{se}/b_0$  (observed) to  $x_{se}/b_0$  (predicted)

$x_d$  is provided as Eq. 1 from the laboratory data:

$$\frac{x_d}{b_0} = 1.7829 \left(\frac{t}{t_e}\right)^{0.56042} (F_d)^{0.5756} \quad (5)$$

It could be observed from Eq. 5, that  $x_d/b_0$  has a direct relationship with  $F_d$  and  $t/t_e$ . There are values of  $RMSE=2.146$  and  $R^2=0.977$  between the calculated and experimental data, which are acceptable. Figure 12 presents the range of changes of  $x_d/b_0$  observations compared to the predicted values from the proposed relationship.

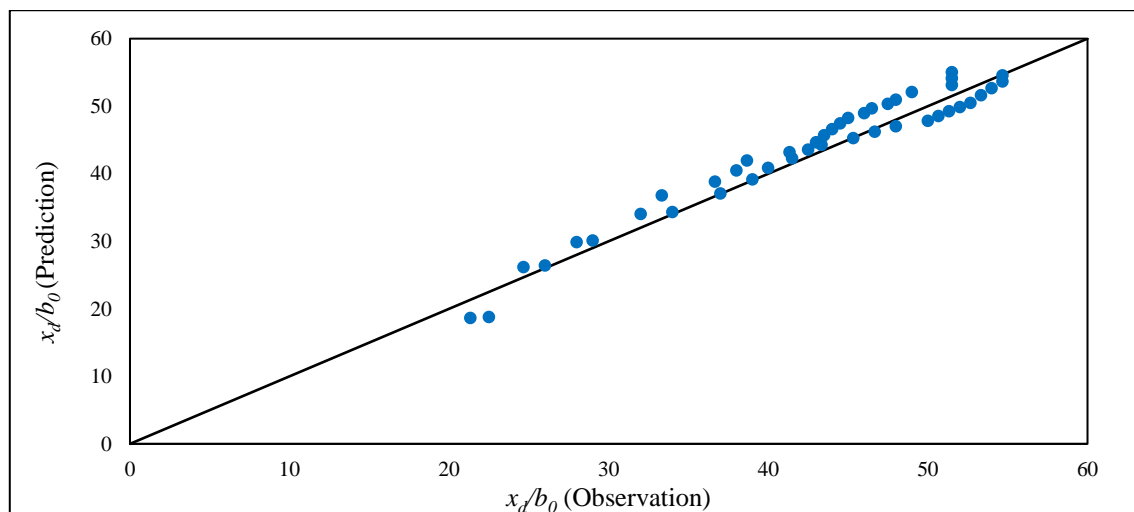


Figure 12. Changes of  $x_d/b_0$  (observed) to  $x_d/b_0$  (predicted)

Table 4 indicates the range of changes in the parameters of the proposed equations.

**Table 4. Variation domain of parameters of proposed equations**

| Equations | Parameter | $F_d$      | $\frac{t}{t_e}$ |
|-----------|-----------|------------|-----------------|
| 1         | $d_{se}$  | 4.97-11.81 | 0.00347-1       |
| 3         | $h_d$     | 4.97-11.81 | 0.00347-1       |
| 4         | $x_{se}$  | 4.97-11.81 | 0.00347-1       |
| 5         | $x_d$     | 4.97-11.81 | 0.00347-1       |

#### 4. Conclusion

In this research, the efficiency of time changes on the scouring profile parameters downstream of sluice gates with  $Fr=1.47$  and  $3.5$  under submerged hydraulic jumps with rigid apron installation in the laboratory has been investigated. These characteristics include the maximum scour depth ( $d_{se}$ ), the maximum dune height ( $h_d$ ), the longitudinal distance of the maximum scour depth from the end of the apron ( $x_{se}$ ), and the longitudinal distance of the maximum dune height from the end of the apron ( $x_d$ ). The maximum values of each characteristic were extracted at different times and their graphs were drawn. The results of the  $d_{se}$  and  $h_d$  time evolution curves indicate that the time variation of depth of scour hole and dune height at the beginning of time is rapid (more than 70% of the final value) and then parameters variation with time became zero and the scour reaches equilibrium condition. According to the time evolution curves of  $x_{se}$  and  $x_d$ , with time, the extension of the location of the maximum scour depth and the dune forms is evident. The experimental data for the dimensionless parameters of the characteristics  $d_{se}/b_0$ ,  $h_d/b_0$ ,  $x_{se}/b_0$ , and  $x_d/b_0$  were analyzed by nonlinear regression method to investigate the effect of time on the values of the characteristics, and separate relationships with  $RMSE=0.045$ ,  $0.0677$ ,  $0.358$ ,  $2.146$  respectively, and  $R^2=0.996$ ,  $0.975$ ,  $0.974$ , and  $0.977$  respectively. These equations show the direct relationship between the characteristic values of  $d_{se}/b_0$ ,  $h_d/b_0$ ,  $x_{se}/b_0$ , and  $x_d/b_0$  with the parameters  $F_d$  and  $t/t_e$ . Also, the range of changes in the parameters of the proposed equations was presented, and the calculated  $R^2$  and  $RMSE$  coefficients present good compatibility between the observed data and the predicted parameters.

## References

1. Balachandar R, Kells JA, Thiessen RJ, (2000). The effect of tailwater depth on the dynamics of local scour. *Canadian Journal of Civil Engineering*, 27, pp: 138-150.
2. Espa P, Sibilla S, (2014). Experimental Study of the Scour Regimes Downstream of an Apron for Intermediate Tailwater Depth Conditions. *Journal of Applied Fluid Mechanics*, 7(4), pp: 611-624.
3. Farhoudi J, Khalili HS, (2014). Investigation on Local Scour Downstream of Adverse Stilling Basins. *Ain Shams Engineering Journal*, 5(2), pp: 361-375.
4. Kells JA, Balachandar R, Hagel KP, (2001). Effect of Grain Size on Local Channel Scour Below a Sluice Gate. *Canadian Journal of Civil Engineering*, 28, pp: 440-451.
5. Dey S, Sarkar A, (2006). Scour Downstream of an Apron Due to Submerged Horizontal Jets. *Journal of Hydraulic Engineering*, 132(3).
6. Dey S, Sarkar A, (2006). Response of Velocity and Turbulence in Submerged Wall Jets to Abrupt Changes from Smooth to Rough Beds and Its Application to Scour Downstream of an Apron. *Journal of Fluid Mechanics*, 556, pp: 387-419.
7. Nik Hassan NMK, Narayanan R, (1985). Local Scour Downstream of an Apron. *Journal of Hydraulic Engineering*, 111(11), pp: 1371-1384.
8. Rajaratnam N, Aderibigbe O, (1993). A Method for Reducing Scour Below Vertical Gates. *Water, Maritime and Energy*, 101(2), pp: 73-83.
9. Hamidifar H, Omid MH, Nasrabadi M, (2010). Bed Scour Downstream of Sluice Gates. *Journal of Water and Soil*, 24(4), pp: 728-736.
10. Hamidifar H, Nasrabadi M, Mirdan AM, Omid MH, (2017). Using a Bed Sill as a Scour Countermeasure Downstream of an Apron. *Ain Shams Engineering Journal*, 9(4), pp: 1663-1669.
11. Hamidifar H, Omid MH, Nasrabadi M, (2018). Reduction of Scour Using a Combination of Riprap and Bed Sill. *Water Management*, 171(5), pp: 264-270.
12. Chaudhary RK, Ahmad, Z, Mishra SK, (2022). Scour downstream of a corrugated apron under wall jets. *Water Practice and Technology*, 17(1), pp: 204-222.
13. Ghassemi A, Nasrabadi M, Omid MH, Estabragh AR, (2022). Effect of synthetic fibers on resisting scour caused by horizontal jet. *Water Science and Engineering*, 15(2), pp:152-160.
14. Ghassemi A, Nasrabadi M, Omid, MH, Raeesi Estabragh A, (2022). Effect of Geonet on Scour Downstream of Horizontal Jets. *Journal of Irrigation and Drainage Engineering*, 148(10), 04022033.
15. Shahsavani Y, Mohajeri SH, Mehraein M, Kisi O, (2022). Prediction of temporal variation of scour hole dimensions due to plane wall jets: Application of new soft computing techniques. *Ocean Engineering*, 251, 111031.
16. Chang CK, Lu JY, Lu SY, Wang ZX, Shih DS, (2020). Experimental and numerical investigations of turbulent open channel flow over a rough scour hole downstream of a ground sill. *Water*, 12(5), 1488.



17. Mostaani A, Azimi AH, (2022). Analytical approach for predicting local scour downstream of submerged sluice gate with an apron. *International Journal of Sediment Research*, 37(4), pp:522-537.
18. Kiani A., *Instructions for irrigation water measurement methods in the field*, 1st edition, Organization of Agricultural Research, Education and Extension, Vice-Chancellor of Extension - Publication of Agricultural Education, Karaj, 2014.
19. Breusers H.N.C., Raudkivi A.J., *Scouring. Hydraulic Structures Design Manual*, 1st Edition, Taylor & Francis Group, 1991.
20. Lim SY, Yu G, (2002). *Scouring Downstream of Sluice Gate*. In 1st International Conference on Scour of Foundations, ICSF-1, Nov. 17-20. Texas A&M University, College Station, Texas, USA.
21. Ali HM, El-Gendy MM, Mirdan, AM, Ali AM, Abdelhaleem, FS, (2014). Minimizing Downstream Scour due to Submerged Hydraulic Jump Using Corrugated Aprons. *Ain Shams Engineering Journal*, 5(4), pp: 1059-1069.
22. Ben Meftah M, Mossa M, (2020). New Approach to Predicting Local Scour Downstream of Grade-Control Structure. *Journal of Hydraulic Engineering*, 146(2).
23. Riahi-Madvar H, Dehghani M, Seifi, A, Salwana, E, Shamshirband, SH, Mosavi A, Chau, KW, (2019). Comparative Analysis of Soft Computing Techniques RBF, MLP, and ANFIS with MLR and MNLR for Predicting Grade-control Scour Hole Geometry. *Engineering Applications of Computational Fluid Mechanics*, 13(1), pp: 529-550.
24. Akbari Dadamahalleh P, Hamidi M, Mahdian Khalili A, (2023). Experimental Prediction of the Bed Profile with the Full-submerged and Semi-submerged Debris Accumulation Upstream of the Cylindrical Bridge Pier. *Journal of Water and Soil Conservation*, 29(4), pp: 95-114.



© 2023 by the authors. Licensee SCU, Ahvaz, Iran. This article is an open access article distributed under the terms and conditions of the Creative Commons Attribution 4.0 International (CC BY 4.0 license) (<http://creativecommons.org/licenses/by/4.0/>).

